

Article

Investigation of Performance and Emission Parameters of Hydroxygen (HHO)-Enriched Diesel Fuel with Water Injection in the Compression Ignition Engine

Romualdas Juknelevičius ^{1,*}, Alfredas Rimkus ², Saugirdas Pukalskas ² and Stanislaw Szwaja ³

¹ Faculty of Mechanics, Vilnius Gediminas Technical University, J. Basanavičiaus g. 28, LT-03224 Vilnius, Lithuania

² Faculty of Transport Engineering, Vilnius Gediminas Technical University, J. Basanavičiaus g. 28, LT-03224 Vilnius, Lithuania; alfredas.rimkus@vilniustech.lt (A.R.); saugirdas.pukaskas@vilniustech.lt (S.P.)

³ Faculty of Mechanical Engineering and Computer Science, Czestochowa University of Technology, 21 Armii Krajowej St., 42-200 Czestochowa, Poland; szwaja@imc.pcz.czyst.pl

* Correspondence: romualdas.juknelevicius@vilniustech.lt; Tel.: +370-5-237-0583

Abstract: The development of engine technologies and research on combustion processes are focused on finding new generation CI engines with simple control of the combustion process while efficiently maintaining desirable engine performance and meeting emission regulations. This comprehensive study on the relatively low hydrogen energy fraction (0.65–1.80%), supplied by onboard water electrolyzers and on water injection, was performed on the performance and emission parameters of the CI engine. The article presents results of both experiment and simulation about the effect of hydroxygen and water injection on the combustion process, auto-ignition delay, combustion intensity, the temperature of the mixture and engine performance at *BMEP* of 0.2 MPa, 0.4 MPa, 0.6 MPa, and 0.8 MPa at a speed of 1900 rpm. For the first part, the test engine operated with diesel fuel with 3.5 L/min of hydroxygen gas supplied with an external mixture formation. The HHO has an effect on the combustion process at all range of *BMEP*. A decrease in *BTE* and increase in *BSFC* were noticed during tests. The peak pressure and the rate of heat release decreased, but the NO_x decreased as well. The second part of experiment was performed with the injection of a substantial amount of water, 8.4–17.4 kg/h (140–290 cm^3/min), and the same amount of hydroxygen. The injection of water further decreased the NO_x ; therefore, HHO and WI can be used to meet emission regulations. A simulation of the combustion process was carried out with the AVL BOOST sub-program BURN. The AVL BOOST simulation provided a detailed view of the in-cylinder pressure, pressure-rise, combustion intensity shape parameter and SOC.

Keywords: hydrogen; hydroxygen; diesel fuel; compression ignition engine; water injection; performance; emission



Citation: Juknelevičius, R.; Rimkus, A.; Pukalskas, S.; Szwaja, S. Investigation of Performance and Emission Parameters of Hydroxygen (HHO)-Enriched Diesel Fuel with Water Injection in the Compression Ignition Engine. *Clean Technol.* **2021**, *3*, 537–562. <https://doi.org/10.3390/cleantechnol3030033>

Academic Editor: Seung-Soo Kim

Received: 20 March 2021

Accepted: 20 July 2021

Published: 26 July 2021

Publisher's Note: MDPI stays neutral with regard to jurisdictional claims in published maps and institutional affiliations.



Copyright: © 2021 by the authors. Licensee MDPI, Basel, Switzerland. This article is an open access article distributed under the terms and conditions of the Creative Commons Attribution (CC BY) license (<https://creativecommons.org/licenses/by/4.0/>).

1. Introduction

The contemporary development of the global economy is closely related to rising power demands and increased power consumption. Fossil fuel resources are the main source of power generation, although it growing use generates global warming. Over the last few decades, the increasing melt process of mountain glacial masses and the ice covers of the North and South Poles have been noticeable. The latter is especially dangerous for the planet, because global sea levels could rise by 60 m if all the ice were to melt. The International Council on Clean Transportation [1] announced that the number of vehicles would reach 1.7 billion in 2030, with the most significant growth in India (+600%), China (+220%) and the Middle East (+161%) in comparison to 2010. In 2017, global CO_2 emissions reached 32.84 eGt CO_2 , while the entire transport fleet reported emissions of 8.04 eGt CO_2 . The CO_2 emissions of road vehicles reached 5.9 eGt CO_2 at that time, which accounts for 73% of the entire transport CO_2 emissions including rail, sea and air fleets [2].

Considering the impact of the well-to-tank (WTT) and tank-to-wheels (TTW) phases, it seems that solar, hydroelectric and wind power are the most appropriate sources to supply the sustainable energy for road transport. However, the short mileage of modern, battery-powered electric vehicles is currently the main obstacle restricting their use. The shortage of hydrogen-fueling stations, combined with the high market price of hydrogen and expensive materials, limits the widespread adoption of FC technology. These issues even more heavily affect heavy-duty vehicles and trucks. Experts predict that, until 2050, hybrid systems with electric and internal combustion engines will be the main powertrains of vehicles. Therefore, the focus on decreasing the emissions of internal combustion engines remains when considering the tank-to-wheel (TTW) phases of hybrid systems.

In 2016–2017, the European Commission announced the Work Programme “*Smart, Green and Integrated Transport*” [3], with an aim to achieve a European transport system that would be resource-efficient, climate friendly and environmentally friendly, with benefits for the economy and society. Research on innovative powertrains and propulsion systems with energy resource efficiency, a reduction in transport dependence on fossil fuels, the take-up of alternative fuels, and the mitigation of climate change, pollution, noise and adverse health effects are the focus points of this program. Further development of engine technologies and research on the combustion processes can boost the break-through in the decrease in emission restrictions.

Potentially, there are only a few chemical substances suitable for achieving the required performance parameters of combustion processes in an internal combustion engine and reducing the emissions. Hydrogen, with its strong thermodynamic and combustion properties and availability across the globe, is one of the most suitable alternative fuels. The use of hydrogen as an energy source has been described by several authors [4–6] discussing long-term scenarios of transition towards clean and sustainable energy. The authors presented a variety of hydrogen-based technologies that allowed for efficient and economically reasonable ways to ensure the global energy demand. The use of the only hydrogen in combustion engines is almost impossible [7–9]; however, co-combustion with other alternative fuels is possible, which therefore makes it the subject of the research interest.

Saravanan [8] and Szwaja [9] performed experiments with only hydrogen combustion in ICE and were faced with problems related to its properties. Saravanan [8] pointed out that hydrogen cannot be used as the sole fuel in a compression ignition (CI) engine, because the compression temperature is not high enough to initiate combustion due to its higher self-ignition temperature. Hence, an ignition source is required while using it in a CI engine. The feasibility investigations of a hydrogen-fueled CI engine with the assistance of a glow plug revealed that glow plug ignition provides reliable ignition and smooth engine operation. The hydrogen ignition delay was very short and the IMEP was higher than the corresponding results obtained with DF. However, significant cycle-to-cycle variations in the ignition delay, associated with the large amplitude pressure oscillations (Szwaja et al. 2010), were observed.

The simple method to use hydrogen in a CI engine is to run it in dual-fuel mode with diesel as the main fuel that acts as an ignition source of hydrogen. However, on-board storage of hydrogen is the obstacle, because in the gaseous form, it can only be stored at the very pressure, which is dangerous. The combination of hydrogen and oxygen gases, named hydroxygen, can be produced with an on-board water electrolysis generator. During this study, a low-performance hydroxygen gas electrolyser was utilized for the laboratory test.

1.1. The Use of Hydrogen in CI Engine

Thermodynamic properties such as low ignition energy, wide flammability limit, and very fast flame propagation rate ensure the prompt ignition of hydrogen [10]. However, safety and storage problems are the challenges of hydrogen use. The molecules of hydrogen are smaller than other gases; therefore, it can diffuse through many materials, including metals, and it can lead to cracks of the metal tank. Such leaks from storage can spark an ignition with an almost-invisible fire, thus leading to accidental burns. This property makes

hydrogen more difficult to store than other gases. The leakage of hydrogen is dangerous, and risks fire when mixed with air. In addition, the challenge of on-board hydrogen storage is the low ratio of the stored hydrogen weight to that of the weight of the whole storage system [11].

The density of the gaseous hydrogen is only 0.0837 kg/m³ and it comprise 6.8% of the air density and 12.8% of the methane density. Even when converted to a liquid state at −252.87 °C, hydrogen is not very dense. The density of liquid hydrogen is 70.8 kg/m³, which is 7% of the density of water. Hydrogen transformed into liquid occupies 848 times less volume than it does in its gaseous state. In fact, because of its close molecular structure and intermolecular bonds of the water, it contains a greater mass of hydrogen than liquid hydrogen itself. One cubic meter contains 111 kg of hydrogen in water, whereas one cubic meter of liquid hydrogen contains only 71 kg of hydrogen.

The LHV of hydrogen (120 MJ/kg) is impressively high in comparison with other fuels: it is more than twice as high as methane and almost three times higher than DF. However, relative parameters such as the gravimetric heating value of a stoichiometric mixture (3.40 MJ/kg) are close to other fuels, whereas the volumetric heating value of a stoichiometric mixture (3.17 MJ/m³) is even lower than that of diesel, gasoline, methane and other fuels. Therefore, with the external (PFI mode) mixture formulation, when hydrogen significantly occupies the volume of the sucked working fluid, the relative performance parameters are considerably modest. The internal mixture formation (DI mode) can lead to a significant increase in performance parameters; however, the injection of hydrogen with DI mode is complicated.

The main properties of the hydrogen and diesel fuel are given in Table 1; an overview of studies of dual-fuel CI engines operating with hydrogen–diesel fuel mixtures is provided below. An overview of dual-fuel CI engines operating with a HHO–diesel fuel mixture with water injection is provided in the following chapters.

Table 1. Fuel properties [8,12,13].

Properties	Diesel Fuel	Hydrogen
Chemical formula	C ₁₀ H ₂₂ –C ₁₅ H ₃₂	H ₂
Composition (wt.%)	84–87 C, 13–16 H	100
Molecular weight	142.3–212.4	2.016
Density at 15 °C and 1.01 bar, kg/m ³	835.3	0.0837
Lower heating value, MJ/kg	42.5	120
Lower heating value, MJ/m ³	36,350	10.7
Stoichiometric air–fuel ratio, kg/kg	14.5	34.2
Heating value of stoichiometric mixture, MJ/kg	2.74	3.40
Heating value of stoichiometric mixture, MJ/Nm ³	3.60	3.17
Minimum ignition energy, mJ	–	0.02
Flammability limits in air at NTP (vol %)	0.6–7.5	4–75
Flame speed, cm/s	30	265–325
Autoignition temperature, °C	250	585

CI engines produce less CO, HC and sulfur oxide during the combustion process of a hydrogen–diesel fuel mixture. However, the co-combustion of hydrogen with diesel leads to a higher speed of combustion and rapid increase in temperature, which results in the increased formation of NO_x and increase in the combustion noise [14]. However, Saravanan et al. [15] noticed that at a hydrogen energy fraction of more than 30%, the NO_x concentration decreased. With the combustion of hydrogen at an energy fraction of less than 30%, an increase from 22.8% to 27.9% of BTE was recorded.

Tests performed by Antunes Gomes et al. [16] demonstrated that the peak in-cylinder pressure was higher in hydrogen-fueled mode due to the higher rate of heat release, although it did not have an unfavorable effect on NO_x formation. The peak temperature was lower in the hydrogen-fueled mode due to the homogeneity of the air–fuel mixture. Tests performed with 20% of HES revealed a decrease in NO_x emissions. The NO_x was

roughly 20% lower than those gained with only diesel operation. When a CI engine is operating at low loads with a lean mixture, the in-cylinder temperature is supposed to be low, as are the NO_x levels (200 ppm). When the load increased, the NO_x levels increased as well.

Subsequent studies with different amounts of hydrogen revealed that emission and performance parameters vary. Zhou et al. [17] tested CI engines with HES values of 10%, 20%, 30% and 40%. An experimental investigation was conducted with naturally aspirated engines at a speed of 1800 rpm under five engine loads. Reductions in p_{max} and peak heat release rate, associated with deteriorations in BTE and BSFC, were observed with the addition of hydrogen under low engine loads due to the low combustion efficiency of hydrogen.

Two combustion modes were observed under heavy engine loads. First, at 70% engine load, three-phase combustion (hydrogen mixing, diesel fuel mixing and diffusion combustion of diesel fuel) occurred with two distinct heat-release jumps. These were associated with a shorter duration of combustion, leading to improvements in BTE and BSFC. Secondly, at 90% engine load, intensive burning with a shorter ignition delay period and shorter combustion duration increased the p_{max} and peak heat release rate, followed by decreases in BTE and BSFC [17].

The use of hydrogen fuel in the mixture has an obvious impact on the performance of CI engine at high loads, because of increases in the p_{max} and peak heat release rate. At the same time, the use of hydrogen improves engine efficiency and reduces CO, CO₂ and PM from medium to high loads [17].

Karagoz et al. [18] examined the performance and emission parameters of CI engines at various loads (40%, 60%, 75% and 100%) with a port supply of hydrogen. NO_x emissions were decreased at all partial engine loads, but a dramatic increase of 51.3% was obtained at full load conditions. The air was excess disclosed as the core factor of the increase in combustion efficiency when hydrogen was supplied with an external mixture formulation.

The presence of hydrogen causes the peak pressure to rise, followed by a temperature rise and increase in NO_x emissions [18], although the addition of hydrogen causes decreases in NO_x at partial loads (40%, 60% and 75%). However, at full load condition (100%), the peak temperature is outweighed and dramatic increases in NO_x emissions are observed.

Experiments carried out with the CI engine [19] at relatively low hydrogen energy fractions of 1.93% reduced in-cylinder pressure, although diminished emissions. The tests were performed at speeds of 1900 rpm and 2500 rpm, a BMEP range of 0.4–0.8 MPa, and hydrogen was supplied into the intake manifold at rates of 10 L/min, 20 L/min, and 30 L/min. The decrease in BSFC, triggered by the presence of hydrogen, was noticed within the whole test range of HES up to 15.74%. The increase in HES shortened the auto-ignition delay and decreased NO_x emissions at both engine speeds.

An investigation [20] was performed on influences of the addition of hydrogen to the CI engine fueled solely with RME and regular diesel fuel sold at a Lithuanian retail outlet, which corresponded to a blend of 7% RME with ULSD. The research focused on combustion phases, ignition delays and exhaust emissions. A decrease in specific fuel consumption was observed, which could be attributed to the higher heating value of the total in-cylinder charge, due to the presence of hydrogen which guided an increase in the combustion temperature. At nominal loads, HES surpassed a 15% increase in NO emissions; however, when HES was less than 15%, the NO emissions decreased at low loads. Further increases in hydrogen fraction were limited and tests were stopped at nominal loads when combustion knock occurred with an HES of nearly 35%.

A summary of the discussed investigations is presented at Table 2 below.

Table 2. Tests performed with hydrogen in a CI engine.

Publication	Test Conditions	H ₂ Supply	Liquid Fuel Supply	BTE	BSFC	NO _x	Smoke	HC	CO
Saravanan et al. [15]		HES > 30%	Diesel fuel			↓		↓	↓
		HES < 30%	Diesel fuel	↑					
Antunes Gomes et al. [16]		HES 20%	Diesel fuel			↓			
Zhou et al. [17]	1800 rpm, 5 loads	HES 10–40%	Diesel fuel	↓	↓				
Karagoz et al. [18]	Loads 40%, 60%, 75%,	H ₂	Diesel fuel			↓			
	100%	H ₂	Diesel fuel			↑			
Juknelevičius et al. [19]	1900 rpm	10 lpm, 20 lpm, 30 lpm	Diesel fuel		↓	↓			
	2500 rpm	10 lpm, 20 lpm, 30 lpm	Diesel fuel		↓	↓			
Juknelevičius et al. [20]		HES > 15%	RME, ULSD + 7% RME			↑			
		HES < 15%	RME, ULSD + 7% RME			↓			

Considering the studies described above, the use of hydrogen reduces NO_x emissions at low loads, but at high loads, NO_x increases.

The use of hydrogen in compression ignition engines of passenger cars is limited due to on-board storage safety issues, related to the low density of hydrogen and high pressure necessary. The most suitable solution to avoid these problems is the production of hydroxygen, composed of hydrogen and oxygen gases, with an on-board water electrolysis generator. However, a drawback of on-board electrolysis generators is the low volumetric efficiency; there is lack of research in this field.

On the basis of the articles reviewed and discussed in Sections 1.2 and 1.3, it can be concluded that there is a gap in the research field of co-combustion of low-volume hydroxygen with diesel fuel in compression ignition engines. The research on the performance and emission parameters of a hydroxygen-enriched diesel fuel with water injection presented in this article can be considered as new knowledge from this point of view.

1.2. The Use of Hydroxygen in CI Engines

The composition of hydroxygen is still an open discussion among researchers [21]. The majority state that HHO gas is a stable cluster composed of hydrogen and oxygen atoms (monoatomic state) and their molecules H₂, O₂ (diatomic state). However, the hypothesis of Santilli [22] states that distilled water at STP occurs via processes structurally different from evaporation or separation mentioned before. Thus, the existence of a new form of water with a structure (H x H)–O was suggested, where “x” represents a new magnecular bond and “–” represents a conventional bond. The transition from conventional H–O–H species to new (H x H)–O species is predicted by changes of the electric polarization of water with an electrolyser. Furthermore, Santilli used the name “HHO gas”. However, Santilli was criticized because there is no scientific evidence that supports the existence of a new form of matter called “HHO gas.” The gaseous product from the electrolyser behaves in the same manner as would be expected of a mixture of hydrogen, oxygen, and therefore could be named hydroxygen.

Nevertheless, there are several articles which use various names of a hydrogen–oxygen blend, i.e., hydroxy (HHO; oxy-hydrogen) by Yilmaz [23] and Arat [24], HHO gas

by Premkartikkumar [25], hydroxyl gas by Masjuki [26], etc. Sometimes, HHO is named Brown gas [27] after Yull Brown (real name Ilia Valkov, 1922–1998), who claimed and patented that HHO could be used as a fuel for ICEs.

However, in this study, hydroxygen was kept as the pure gas mixture with a 2:1 molar ratio of hydrogen and oxygen gases.

Yilmaz et al. [23] used HHO gas as a supplementary fuel in a CI engine. The increase in engine torque output with a mean value of 19.1% and a 14% decrease in BSFC was observed when hydroxygen was supplied to the engine. The reductions in emissions were CO by 13.5%, and HC by 5%. However, at low engine speeds, advantages of HHO turned into disadvantages for engine torque, CO, HC emissions and BSFC.

Arat et al. [24] tested HHO and CNG mixtures in CI engines with pilot diesel injection. Three experiments were performed: in the first case, sole diesel operation; in the second case, there was a supply of 5.1 L/min of HHO addition; and in the third case, a mixture of 25% HHO (5.1 L/min) and 75% CNG (15.3 L/min) was introduced to the intake manifold. The average BTE improved using HHO by 3.4%, and using HHO+CNG was 6.28% better than base diesel operation. The use of HHO decreased the CO emissions by 15% and CO₂ emissions by 9.03%. However, higher burning temperatures of HHO lead to increases in NO_x emissions.

Baltacioglu et al. [28] compared the performance and emission characteristics of a pilot-injection diesel engine with the addition of hydrogen or HHO. The ULSD was blended with biodiesel at a volumetric ratio of 10%. Additionally, intake air was fed with pure hydrogen or hydroxygen. The hydrogen was supplied to the engine at a rate of 10 L/min. The performance indicators and exhaust emissions were improved, except for NO_x. The increases in NO_x emissions were 20% with HHO and 16% with H₂. In comparison with pure diesel fuel, CO emissions were reduced by 29% with H₂ and by 22% with HHO. It was highlighted that the supply of HHO has higher engine performance results in comparison to H₂.

Masjuki et al. [26] introduced HHO gas with a blend of ULSD and 20% palm biodiesel to evaluate the engine performance and emission characteristics. The presence of HHO reduced the CO, because the high combustion temperature facilitated CO conversion to CO₂, which therefore showed lower HC emissions. However, the presence of HHO influenced the high rate of heat release produced by the oxidation of hydrogen and increase in NO emissions by an average of 25%.

Mustafa et al. [29] investigated CI engines fueled with a hydrogen- or HHO (10 L/min)-enriched Castor oil methyl ester–diesel fuel blend with a 20% volumetric ratio (CME20). Hydrogen or HHO were supplied with an external mixture formulation, using a mix chamber positioned before entry to the intake manifold. The engine was tested at speeds between 1200 rpm and 2600 rpm. The brake power improved by 4.3% with HHO+CME20, whereas H₂+CME20 fuel resulted in an average increase of 2.6% compared to that of pure diesel fuel. The addition of sole hydrogen to CME20 had a better effect on exhaust gas emissions compared to that with the addition of HHO. The CO emissions were reduced by up to 27% with H₂+CME20 and up to 21% with HHO+CME20.

Tests with small amounts (3.3 L/min) of HHO gas increased the brake thermal efficiency by 11.06% [25]. The CO emissions decreased by 15.38% and smoke reduced substantially by 26.19%, although increases in CO₂ by 6.06% and NO_x by 11.19% were registered during experiments performed with a four-stroke, direct-injection CI engine, developing a rated power of 5.9 kW at a speed of 1800 rpm.

However, with smaller amounts of 1 L/min of HHO gas, the brake thermal efficiency decreased by 4.15%. The NO_x emissions decreased by 15.48%, although the smoke and CO emissions increased by 7.69%.

Laboratory investigations by Rimkus [27] focused on the influence of HHO gas upon the energy and performance indicators of CI engines. A power generator of the test CI engine was employed to supply energy for the water electrolyser. Therefore, the electrolyser-generated HHO reduced the maximum brake torque by 2.6–2.7% and increased

the indicated specific fuel consumption by up to 2%. However, HHO improved the combustion and reduced the exhausts: CO emissions decreased by 15%, HC emissions decreased by 9%, and the smokiness decreased by 25%.

Investigations of low hydroxygen fractions [30] on diesel engines with EGR were carried out at an engine speed of 2000 rpm and brake torque of 45 Nm. The engine specific fuel consumptions increased and efficiency decreased by 1.4% with a supply of HHO gas of 3 L/min. This volume corresponds to a hydrogen energy share of 1.06%.

A summary of these investigations is presented at Table 3 below.

Table 3. Tests performed with hydroxygen in CI engines.

Publication	Test Conditions	HHO Supply	Liquid Fuel Supply	BTE	BSFC	NO _x	Smoke	HC	CO
Yilmaz et al. [23]		HHO	Diesel fuel		↓			↓	↓
Arat et al. [24]		5.1 lpm HHO	Diesel fuel	↑		↑			↓
		5.1 lpm HHO + 15.3 lpm CNG	Diesel fuel	↑		↑			↓
Baltacioglu et al. [28]		10 lpm HHO or H ₂	ULSD + 10% biodiesel	↑	↓	↑		↓	↓
Masjuki et al. [26]		HHO	ULSD + 20% biodiesel			↑		↓	↓
Mustafa et al. [29]	1200–2600 rpm	10 lpm HHO or H ₂	ULSD + 20% biodiesel	↑					↓
Premkartikkumar et al. [25]	5.9 kW 1800 rpm	1 lpm HHO	Diesel fuel	↓		↓	↑		↑
		3.3 lpm HHO	Diesel fuel	↓		↑	↓		↓
Rimkus [27]		1.5 lpm HHO	Diesel fuel	↓			↓	↓	↓
Rimkus et al. [30]	45 Nm 2000 rpm	3 lpm HHO	Diesel fuel	↓	↑				

A review of the literature on previous experimental tests indicates that a supply of hydroxygen suggests certain improvements in engine performance indicators due to the spontaneous ignition of hydrogen, unless increases in NO emission are noticed. Water injection could reduce the spontaneous ignition of hydrogen, decrease NO_x emissions and better balance the combustion process.

1.3. Water Injections in CI Engines

A broad range of experimental studies on water injection into the intake manifold of CI engine were carried out by Tesfa et al. [31]. The test engine worked with biodiesel and WI in the following engine speed–load matrix. The WI rates were 0 kg/h, 1.8 kg/h, 3 kg/h, engine speeds were 900 rpm, 1100 rpm, 1300 rpm and 1500 rpm, and engine loads were 105 Nm, 210 Nm, 315 Nm and 420 Nm. The peak in-cylinder pressure and rate of heat release of various tests only had marginal magnitude differences for various WI rates at the given operating conditions. The WI did not induce any significant changes in the BSFC or BTE of the engine at medium or high engine loads. Only at a low load of 105 Nm were a 4% increase in BSFC and a 3% decrease in BTE observed.

The results show that the WI affects the premixed combustion temperature which occurs at a combustion of 0–10% MFB and mainly causes NO_x emissions. However, the NO_x emissions were reduced by up to 50% over the entire operating range. Therefore, it was concluded that WI can be employed to reduce NO_x emissions without loss of power or any negative effects on fuel consumption.

Tauzia et al. [5] performed an experimental study on high-speed common-rail diesel engines in order to measure the effects of water injection on the combustion process and emissions. The experimental study revealed significant reductions in NO_x emissions with high WI rates at low and high loads. It was concluded that with a water mass of about 60–65% of that of fuel mass, it was possible to obtain a 50% reduction in NO_x.

The study performed by Adnan et al. [32] was an attempt to optimize the initiation and duration of WI on CI engines running on a diesel fuel and hydrogen mixture. Water at a pressure of 2 bars was injected, from 20° BTDC to 20° ATDC, with injection durations of 20° CA and 40° CA. This corresponds to 0.42 kg/h (7 cm³/min) and 0.86 kg/h (14 cm³/min) doses. The engine was tested at different loads and speeds: 4 kW at 1500 rpm, 3 kW at 2000 rpm, 2 kW at 2500 rpm, and 1 kW at 3000 rpm.

The engine ITE of a CI engine running on a diesel fuel–hydrogen mixture with WI was higher than one using only diesel fuel. Maximum ITE (42%) was achieved at a load of 3 kW at 2000 rpm and WI of 0.42 kg/h at 20° BTDC. Injection of 0.86 kg/h of water at 20° ATDC reached the maximum heat release of 79.32 J/deg, although a higher ROHR was received without water injection with the engine running on a diesel–hydrogen mixture.

Higher NO_x emissions were measured with a WI duration of 40° CA corresponding to a water flow rate of 0.86 kg/h as compared to 20° CA duration. It was concluded that a higher decrease in NO_x emissions is related to higher water flow rates. This is because more water droplets introduced into the cylinder reduce the in-cylinder charge temperature, and thus lower the emissions of nitrogen oxides. The WI system with optimized injection timing can be used to enhance the engine performance and decrease emissions.

The study of Chintala and Subramanian [33] aimed to reduce NO_x emissions with a supply of hydrogen and injections of various amounts of water. The tests were performed with a single-cylinder CI engine with an output of 7.4 kW at 1500 rpm using a diesel–biodiesel blend (B20) and H₂. The hydrogen was sprayed at 3 bars of pressure and water was injected with a pressure of 2 bars into the intake manifold. Tests were carried out with such SWC values of 130 g/kWh, 200 g/kWh and 270 g/kWh, which corresponded to 32%, 36% and 39% of hydrogen energy value of the mixture, respectively.

Due to the water supply, the p_{max} , peak temperature, and ROHR decreased. The ignition delay and combustion duration increased, because the ignition in the combustion chamber started later with a longer combustion duration. The supply of 200 g/kWh of water with 36% of HES provided the lowest emissions and the maximum power. The maximum NO_x reduction, 37%, was achieved with an SWC of 270 g/kWh, with slight increases in the other pollutants (HC, CO and smokiness).

A further study performed by Chintala and Subramanian [34] dealt with combined effects. Enhancement of the hydrogen energy fraction was tested along with water injection and the change in CR. The SWC varied from 130 to 480 g/kWh. Tests were performed with a 7.4 kW rated CI engine at 1500 rpm. The CR was adjusted to the following values: 19.5:1, 16.5:1 and 15.4:1.

The BTE under dual-fuel mode increased remarkably with increases in HES as compared to the solely diesel fuel mode with a CR of 19.5:1. With increased SWC and reduced CR, the thermal efficiency was lower than that of conventional dual-fuel mode; however, at a CR of 16.5:1 and SWC of 340 g/kWh, the efficiency was comparable with base diesel mode efficiency.

The HES was increased to 66.5% with an SWC of 480 g/kWh, and to 79% with a combined control strategy (SWC of 340 g/kWh and CR of 16.5:1). The combined control strategy of CR of 16.5:1 and SWC of 340 g/kWh decreased the p_{max} .

HC, CO, smokiness and NO_x emissions decreased significantly with the combined control strategy as compared to pure diesel mode, although were slightly higher than the conventional dual-fuel mode. The notable conclusion raised from this study was that a combined strategy of water addition and CR reduction is a promising solution for the enhancement of maximum HES and possible reductions in NO_x emissions.

Taghavifar et al. [35] used the computational CFD package AVL-FIRE to study how WI can suppress knocking and intensive heating, which lead to increases in NO_x emissions. A Ford 1.8 l HSDI-type CI engine model was considered to study the effect of WI. In this investigation, the water was injected with volume fractions of 5%, 10%, and 15% of the total fuel mixture.

The peak of the ROHR increased from 22.83 J/deg to 34.82 J/deg in sole diesel mode compared with the 15% water volume fraction of the total fuel mixture. The peak of the ROHR rose from 25.096 J/deg of pure hydrogen to 28.5 J/deg of hydrogen with a water volume fraction of 15% of the total fuel mixture. However, employing WI, a significant reduction in the in-cylinder temperature was achieved. The peak in-cylinder temperature decreased from 2100 K to 1300 K, corresponding to pure hydrogen with the WI case. The highest peak pressure and indicated torque, denoting thermal efficiency and engine power, respectively, were observed with a water fraction of 15% of the total fuel mixture by volume. In contrast, the lowest NO_x emissions were achieved when diesel and hydrogen fuels were combusted with a WI of 5% of the total fuel mixture fraction.

The findings of the above investigations are summarized in Table 4.

Table 4. Tests performed with water injection in CI engines.

Publication	Test Conditions	H ₂ Supply	Liquid Fuel and Water Supply	BTE	BSFC	NO _x	Smoke	HC	CO
Tesfa et al. [31]	900–1500 rpm 105–420 Nm	No H ₂ supply	Diesel fuel WI 0.8–3 kg/h	↓	↑	↓			
Tauzia et al. [5]		No H ₂ supply	Diesel fuel WI 60–65 wt.% of fuel			↓			
Adnan et al. [32]	1–4 kW 1500–3000 rpm	H ₂	Diesel fuel WI 0.42–0.86 kg/h			↓			
Chintala et al. [33]	7.4 kW 1500 rpm	HES 32–39	ULSD + 20% biodiesel WI 130–270 g/kWh			↓	↑	↑	↑
Chintala et al. [34]	7.4 kW 1500 rpm Comp. ratio 15.4–19.5	HES 32–39	ULSD + 20% biodiesel WI 130–480 g/kWh			↓	↓	↓	↓
Taghavifar et al. [35]		H ₂	ULSD WI 5–15% of fuel vol			↓			

The homogeneity of hydrogen–air mixtures remarkably deteriorated compared to that of diesel fuel–air mixtures when water was injected. Therefore, with water injection, reductions in in-cylinder pressure and temperature can be obtained.

2. Research Equipment and Test Methodology

The present research was carried out to analyze the effect of HHO injection on the combustion, performance and emissions parameters of CI engines running on pure diesel fuel and how HHO affects the combustion of diesel fuel with the injection of water.

Experiments were performed at the Laboratory of Transport Engineering and Logistics of Vilnius Gediminas Technical University. A diesel engine with a turbocharger, electronically controlled BOSCH VP37 fuel pump and conventional mechanical fuel injection was used for tests. The technical specifications of the test engine are presented in Table 5.

The installation of the test bed is shown in Figure 1. The diesel engine (1) was connected to a dynamometer, KI-5543 (2), to manage and monitor the engine speed and load.

The engine was set to operate at a speed of 1900 rpm. Each experiment was performed at fixed loads of 30 Nm (corresponding to $BMEP = 0.2$ MPa), 60 Nm ($BMEP = 0.4$ MPa), 90 Nm ($BMEP = 0.6$ MPa), and 120 Nm ($BMEP = 0.8$ MPa). The fixed loads were controlled by adjustment of the diesel fuel mass flow rate.

Injections of diesel fuel with different timings of SOI were applied with various engine speed and $BMEP$ values. The following diesel fuel injection timings were set: SOI = 2° BTDC with $BMEP = 0.2$ MPa; SOI = 2.5° BTDC with $BMEP = 0.4$ MPa; SOI = 3° BTDC with $BMEP = 0.6$ MPa; and SOI = 4° BTDC with $BMEP = 0.8$ MPa.

The torque measurement error was ± 1.23 Nm. Diesel fuel consumption was measured using a sensitive electronic scale SK-5000 (12 in Figure 1). The accuracy of the fuel

consumption measurement was 0.5%. Pollutants of the exhaust gas were analyzed with AVL DiSmoke (9) and AVL DiCom 4000 (10) analyzers. The measurement ranges and accuracies of the AVL DiCom 4000 gas analyzer are given in Table 6.

Table 5. Parameters of test engine.

Parameter	Value
Number of cylinders	4
Cylinder bore, mm	79.5
Piston stroke, mm	95.5
Displacement, cm ³	1896
Compression ratio	19.5
Length of connecting road, mm	150
Maximum engine power, kW	66 @ 4000 rpm
Maximum engine torque, Nm	180 @ 2000–2500 rpm
Inlet valve open	16° BTDC
Inlet valve close	25° ABDC
Exhaust valve open	28° BBDC
Exhaust valve close	19° ATDC

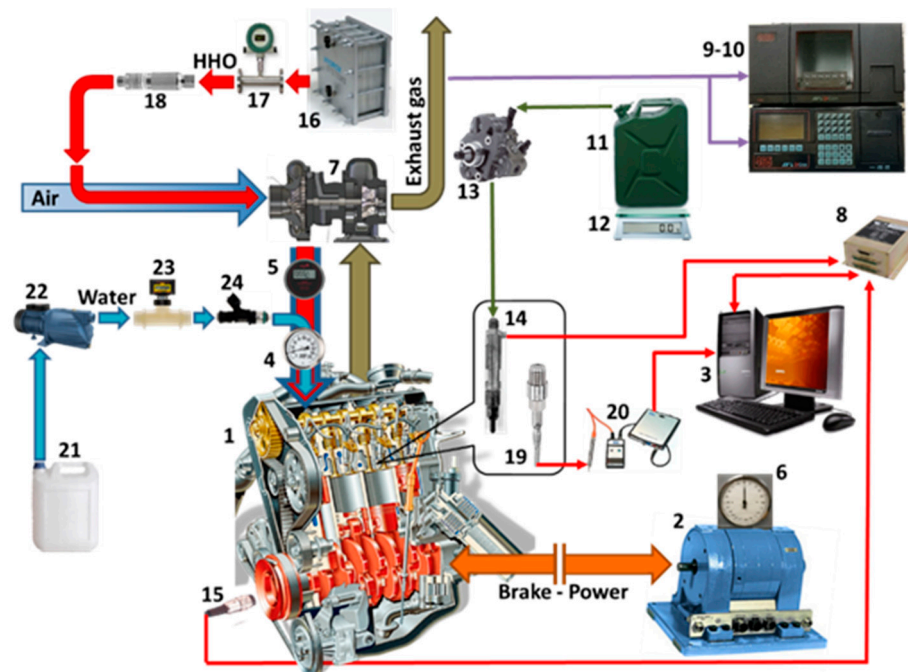


Figure 1. The scheme of engine test equipment: 1—diesel engine; 2—dynamometer; 3—computer; 4—thermometer; 5—air pressure meter; 6—engine torque and rotation speed meter; 7—turbocharger; 8—data acquisition system; 9—smokiness analyzer; 10—exhaust gas analyzer; 11—fuel tank; 12—fuel consumption scale; 13—high-pressure fuel pump; 14—fuel injector; 15—crank angle encoder; 16—HHO gas generator; 17—HHO gas flow meter; 18—HHO gas flashback arrestor; 19—in-cylinder pressure sensor; 20—amplifier and data reading; 21—water tank; 22—water pump; 23—water flow meter; 24—water injector.

Table 6. Measurement ranges and accuracies of the AVL DiCom 4000 gas analyzer.

Parameter	Measurement Range	Accuracy
NO _x	0–5000 ppm	1 ppm
HC	0–20,000 ppm	1 ppm
CO	0–10% vol	0.01% vol
CO ₂	0–20% vol	0.1% vol
O ₂	0–25% vol	0.01% vol
Absorption (K-Value)	0–99.99 m ⁻¹	0.01 m ⁻¹

In the present study, the hydrogen with oxygen was produced by water electrolysis. An electrolyser (Figure 2a) used an electric current to dissociate the water molecules into hydrogen and oxygen, creating hydroxygen (HHO) gas. This feasible solution for hydrogen production avoids the storage of hydrogen in heavily pressurized tanks and can be installed on-board vehicles. The hydroxygen itself is a combustion mixture, already containing the reactant (hydrogen) and the oxidizer (oxygen). In fact, the stoichiometric ratio of HHO for the oxygen–hydrogen mixture, according to the combustion reaction $2\text{H}_2 + \text{O}_2 \rightarrow 2\text{H}_2\text{O}$, is:

$$\frac{1\text{mol}(\text{O}_2)}{2\text{mol}(\text{H}_2)} = \frac{32\text{g}}{4.032\text{g}} = 7.94 \quad (1)$$



(a)



(b)

Figure 2. The water electrolyser (a) and AEM water injection kit with a pressure pump (b).

During electrolysis, 1 kg water is transformed into the gas mixture, which has almost sufficient fractions of oxygen (887 g) and hydrogen (113 g) for stoichiometric combustion. Consequently, external oxygen is not required for combustion. The ratio of the oxygen–hydrogen mixture obtained during the electrolysis of 1 kg water is:

$$\frac{887\text{g}}{113\text{g}} = 7.84 \quad (2)$$

The water electrolyser used a direct current to produce the HHO gas. Direct current was supplied by an external power source. HHO gas consists of two-thirds hydrogen and one-third oxygen by volume, and its components are not separated.

In the first part of the test, the engine was operated using diesel fuel (D) and a D+HHO mixture. The HHO gas at a volume flow rate of 3.5 L/min, corresponding to a mass flow rate of 0.0125 kg/h (Table 7), was introduced in front the turbocharger with an external mixture formulation. The HHO was supplied permanently to ensure better gas distribution and homogeneity of the mixture. The HES decreased from 1.80% to 0.66% with an increase in *BMEP*.

Table 7. The amounts of HHO and water supplied during various modes of the test.

Indicators	D+HHO	D+H ₂ O	D+HHO+H ₂ O
		<i>BMEP</i> = 0.2 MPa	
HES, %	1.80	–	1.69
Mass flow rate of HHO, kg/h	0.0125	–	0.0125
Mass flow rate of H ₂ O, kg/h	–	8.4	8.4
		<i>BMEP</i> = 0.4 MPa	
HES, %	1.16	–	1.13
Mass flow rate of HHO, kg/h	0.0125	–	0.0125
Mass flow rate of H ₂ O, kg/h	–	11.2	11.2
		<i>BMEP</i> = 0.6 MPa	
HES, %	0.84	–	0.81
Mass flow rate of HHO, kg/h	0.0125	–	0.0125
Mass flow rate of H ₂ O, kg/h	–	13.4	13.4
		<i>BMEP</i> = 0.8 MPa	
HES, %	0.66	–	0.65
Mass flow rate of HHO, kg/h	0.0125	–	0.0125
Mass flow rate of H ₂ O, kg/h	–	15.0	15.0

In the second part, experiments were repeated according to the aforementioned procedures with the injection of water (D+H₂O and D+HHO+H₂O). The AEM water injection kit with a pressure pump (Figure 2, right) was installed after the turbocharger and before the intake manifold to supply the homogenized mixture of air and water droplets. The water mass flow rate varied from 8.4 to 17.4 kg/h (Table 7), depending on the *BMEP* and engine speed. The air compressed by the turbocharger was used to vaporize the water and produce an atomized mist.

In-cylinder pressure was measured with a piezo sensor GG2-1569 (Figure 1, position 15) and recorded using AVL DiTEST DPM 800 equipment (19). The pressure measurement accuracy was 1%. The pressure in the intake manifold of the engine, measured with a Delta OHM HD 2304.0 pressure gauge (5), had a measurement error of ± 0.0002 MPa. The temperature of the exhaust manifold T_m was determined by an infrared thermometer Emsitest IR 8839, with a precision of ± 1.5 °C.

The LHV of the fuel mixture was calculated with the formula:

$$H_{L,mix} = \frac{H_{L,D} \cdot C_{m,D}}{100} + \frac{H_{L,H2} \cdot C_{m,H2}}{100} \quad (3)$$

where $H_{L,D}$ is the LHV of the diesel fuel, 42.5 MJ/kg; $H_{L,H2}$ is the LHV of the hydrogen, 120 MJ/kg (Table 1); $C_{m,D}$ is the mass fraction of the diesel fuel in the mixture %; and $C_{m,H2}$ is the mass fraction of the hydrogen in the mixture, %.

The mass fraction of the diesel fuel, %, is:

$$C_{m,D} = \frac{m_{c,D} \cdot 100}{m_{c,D} + m_{c,H2}} \quad (4)$$

where $m_{c,D}$ is the cyclic mass flow rate of the diesel fuel, g/cycl; and $m_{c,H2}$ is the cyclic mass flow rate of the hydrogen, g/cycl.

The mass fraction of the HHO gas, %, is:

$$C_{m,HHO} = \frac{m_{c,H2} \cdot 100}{m_{c,D} + m_{c,H2}} \quad (5)$$

The cyclic mass flow rate of the diesel fuel, g/cycl, is:

$$m_{c,D} = \frac{B_D \cdot 1000 \cdot \tau}{60 \cdot 2 \cdot n \cdot i} \quad (6)$$

where B_D is the mass flow rate of the diesel fuel, kg/h; τ is the number of engine strokes; n is the engine speed, rpm; and i is the number of cylinders of the engine.

The cyclic mass flow rate of the hydrogen, g/cycl, is:

$$m_{c.H2} = \frac{B_{H2} \cdot 1000 \cdot \tau}{60 \cdot 2 \cdot n \cdot i} \quad (7)$$

where B_{H2} is the mass flow rate of the hydrogen, kg/h:

$$B_{H2} = \frac{Q_{HHO} \cdot \rho_{HHO} \cdot 60}{1000} \quad (8)$$

where Q_{HHO} is the volume of HHO gas supplied to the engine, m³/h; and ρ_{HHO} is the density of the HHO gas, 0.54 kg/m³.

The combustion synthesis was simulated with AVL BOOST. Pressure, pressure-rise, ROHR traces, SOC, CD and m_v , estimated by the AVL BOOST sub-program BURN, are presented and discussed in Section 4.

Error Analysis

Errors and uncertainties occurred during the performed tests due to inaccuracies in the calibrations of measuring equipment and in the observations. Uncertainties of the performed tests were determined following Holman [36]. The result, R , of the performed tests is expressed with the function:

$$R = a_1 x_1 + a_2 x_2 + \dots + a_n x_n \quad (9)$$

where R is the result of the function; $x_1, x_2, x_3, \dots, x_n$ are independent variables of the function; and $a_1, a_2, a_3, \dots, a_i$ are partial derivatives of independent variables:

$$\frac{\partial R}{\partial x_i} = a_i \quad (10)$$

The uncertainties of the result R are expressed as:

$$\Delta R = \left[\left(\frac{\partial R}{\partial x_1} \Delta x_1 \right)^2 + \left(\frac{\partial R}{\partial x_2} \Delta x_2 \right)^2 + \dots + \left(\frac{\partial R}{\partial x_n} \Delta x_n \right)^2 \right]^{\frac{1}{2}} = \left[\sum_{i=1}^n \left(\frac{\partial R}{\partial x_i} \right)^2 \Delta x_i^2 \right]^{\frac{1}{2}} \quad (11)$$

where ΔR is the uncertainty of the result; $\Delta x_1, \Delta x_2, \dots, \Delta x_n$ are uncertainties of the independent variables; R is the result of the function; and $x_1, x_2, x_3, \dots, x_n$ are independent variables of the function.

Using Equation (9), the uncertainty of test results such as in-cylinder pressure, $BMEP$, and BTE were determined to prove the accuracy of the experiment. The engine speed, n , and LHV considered as accurate values; therefore, they did not influence the measured values.

The uncertainty of the in-cylinder pressure is dependent on errors of the pressure transducer and amplifier, and the uncertainty of data acquisition:

$$\Delta p = \left[\Delta p_t^2 + \Delta a^2 + \Delta a_m^2 \right]^{\frac{1}{2}} \quad (12)$$

where Δp is the uncertainty of in-cylinder pressure; Δp_t is the uncertainty of the pressure transducer; Δa is the uncertainty of the amplifier; and Δa_m is the uncertainty of the data acquisition module.

The uncertainty of the $BMEP$ can be determined from Equation (11):

$$\Delta BMEP = \left[\Delta p^2 + \Delta V^2 \right]^{\frac{1}{2}} \quad (13)$$

where $\Delta BMEP$ is the uncertainty of the $BMEP$; Δp is the uncertainty of in-cylinder pressure; and ΔV is the uncertainty of instantaneous cylinder displacement.

The uncertainty of the *BTE* is as follows:

$$\Delta BTE = \left[\Delta BMEP + \Delta B_D^2 + \Delta B_{H_2}^2 \right]^{\frac{1}{2}} \quad (14)$$

where ΔBTE is the uncertainty of the *BTE*; $\Delta BMEP$ is the uncertainty of the *BMEP*; ΔB_D is the uncertainty of the mass flow rate of diesel fuel; and ΔB_{H_2} is the uncertainty of the mass flow rate of HHO.

Uncertainties of the in-cylinder pressure, engine torque, *BSFC*, and *BTE* are given in Table 8.

Table 8. The uncertainty of parameters measured during the test.

Parameters	Uncertainty, %
In-cylinder pressure, p	± 1
Engine torque, M_e	± 1
<i>BMEP</i>	± 1.2
<i>BSFC</i>	± 2.5
<i>BTE</i>	± 2.3

3. Results and Discussion

3.1. Performance Analysis

The peak pressure, p_{max} , was lower when the engine was fed with a D+HHO mixture in comparison to the results when the engine was fed with pure diesel fuel (Figure 3). The density of hydrogen is extremely low. The volumetric heating value of the stoichiometric hydrogen–air mixture was 3.17 MJ/m³, which was roughly 88% of that of a diesel–air mixture (Table 1). The tests were performed with air excess ratios of 1.9–4.6. Thus, the volumetric heating value of the HHO–air mixture was even lower than the stoichiometric mixture, particularly at a low load. Therefore, the in-cylinder pressure and power output were reduced in the dual-fuel mode in comparison to that of the solely diesel mode; Gomes Antunes et al. [16] reported similar results. The lowest *BSFC* (Figure 4) and the highest *BTE* (Figure 5) were obtained when the engine operated solely with diesel fuel. The *BSFC* increased and *BTE* decreased when the engine ran on a D+HHO mixture.

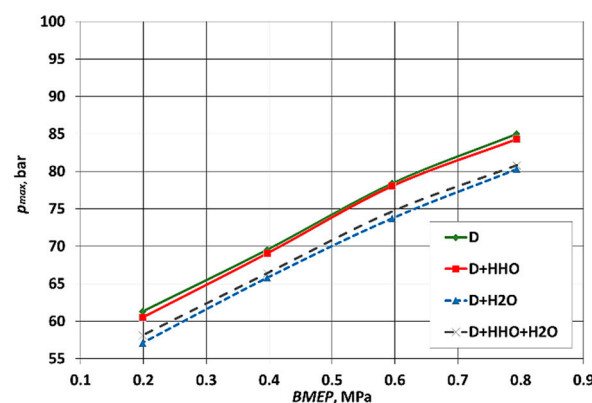


Figure 3. In-cylinder maximum pressure vs. *BMEP* with various fuel mixtures (and water injection).

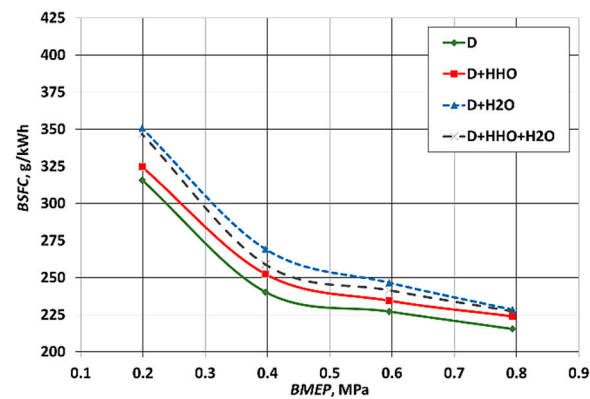


Figure 4. The BSFC vs. BMEP with various fuel mixtures (and water injection).

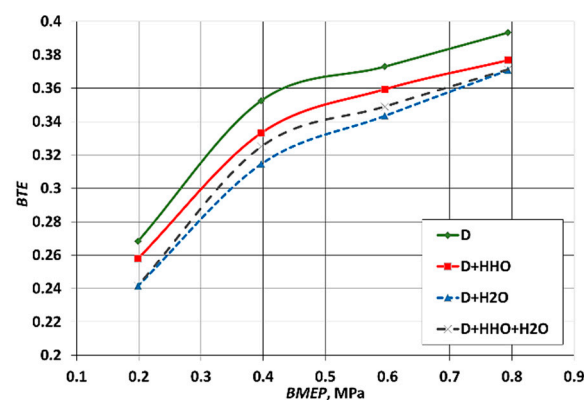


Figure 5. The BTE vs. BMEP with various fuel mixtures (and water injection).

The other reason for lower performance with the D+HHO mode is a shortened auto-ignition delay. The shorter auto-ignition delay reduced the heat released in the pre-mixed combustion phase, reduced the peak pressure p_{max} , and reduced the NO_x emissions. Szwaja et al. [9], after investigation of a CI engine with small amounts of hydrogen (about 5%), noticed that the injection of H_2 shortened the diesel auto-ignition delay and decreased the rate of pressure increase. Research by Zhou et al. [17] confirmed the effect of poorer engine performance with hydrogen fractions of 10–40% at low BMEP values of 0.08 MPa and 0.25 MPa at 1800 rpm. It was determined that such an effect is due to the low combustion efficiency of hydrogen under low engine loads, which was indicated by the decrease in p_{max} . Saravanan et al. [7] also demonstrated that a relatively small amount of H_2 (<5% of HES) reduced the BTE at low engine loads.

In-cylinder peak pressure diminished significantly when the engine used D+ H_2O and D+HHO+ H_2O at both engine speeds. The drop in the peak pressure was due to the loss of heat. Part of the heat was consumed in heating and evaporating the cold water. This loss of heat consequently decreased the temperature of compressed air, in-cylinder pressure at the end of compression, and the peak pressure. This fact was revealed in a study by Adnan et al. [32] with a CI engine with different WI timings and durations. The presence of water droplets inhibits the start of premixed combustion, reduces the flame velocity, and reduces the peak pressure.

When the engine was fed with a D+HHO+ H_2O mixture, the temperature in the combustion chamber decreased and BSFC increased because of the higher diesel fuel mass flow rate required to keep the BMEP steady, in accordance with the test matrix. The fixed loads were controlled by adjustment of the diesel fuel mass flow rate. The evidence of this was the further increase in diesel fuel consumption in comparison with the D and D+HHO mode.

The reduction in heat released in the pre-mixed combustion phase was followed by decreases in the flame speed. Additionally, outspread of the flame throughout the combustion chamber was stopped near to the walls of the combustion chamber due to quenching, which was caused by the presence of HHO [37].

The simulation of the in-cylinder pressure using the Vibe combustion model of the AVL BOOST presented in Section 4, showed similar trends.

3.2. Emissions Analysis

The NO_x was reduced by 3–4% (Figure 6) when HHO gas was fed into the engine along with diesel fuel. As discussed by Lee et al. [38], this reduction in NO_x is the result of a diminished auto-ignition delay and reduced heat release in the pre-mixed combustion phase. The low fraction of hydrogen fed into the combustion chamber initiates faster combustion at the pre-mixed phase, but this phenomenon leads to a shorter combustion duration of the mixture and decreases the gas expansion energy. Therefore, to maintain the required *BMEP*, the cyclic amount of diesel fuel must be increased; thus, increases in *BSFC* were observed (Figure 4). Co-combustion of the HHO with diesel fuel improved the intensity of combustion, but shortened the process.

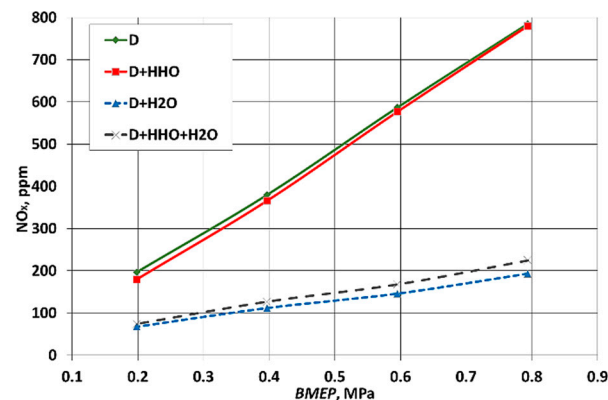


Figure 6. NO_x emissions vs. *BMEP* with various fuel mixtures (and water injection).

When the engine was fed with a D+HHO+ H_2O mixture, the NO_x decreased further. At a *BMEP* of 0.2 MPa, NO_x decreased more than twice when compared to diesel alone, and at the highest load of *BMEP* 0.8 MPa, it dropped 3–4-fold. The high heat vaporization of water reduced the combustion temperature. At a *BMEP* of 0.4 MPa, the temperature decreased by 40 K compared with D and D+ H_2O , and 45 K compared with D+HHO and D+HHO+ H_2O at the TDC. At a *BMEP* of 0.6 MPa, the temperature decreased by 48 K compared with D and D+ H_2O , and 54 K compared with D+HHO and D+HHO+ H_2O at the TDC. The water vapor in the combustion chamber decreased the temperature and increased the heterogeneity of the mixture. The formation of NO_x is affected not only by the duration of combustion, as it discussed in the case of the D+HHO mode, but by temperature as well, as observed in the case of water injection. Therefore, both parameters, combustion duration and temperature, have an influence on the formation of NO_x .

Prabhakumar et al. [39] also concluded that lower levels of NO_x emissions were observed due to the diminished combustion temperature, highly reduced ignition delay phase, and the reduced ROHR in the pre-mixed combustion phase.

Due to WI, the reduction in the temperature increased the cyclic amount of diesel to obtain the required *BMEP* and significantly increased smokiness (Figure 7), especially at a *BMEP* of 0.6 MPa and a *BMEP* of 0.8 MPa. Higher loads require more fuel, but the injection of water decreases the temperature to such a level that part of fuel is not burned properly and is exhausted. Thus, significant increases in smokiness were observed at higher loads: *BMEP* 0.6 MPa and *BMEP* 0.8 MPa.

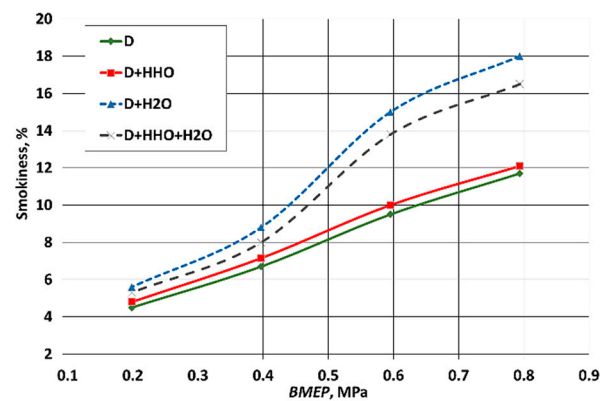


Figure 7. The smokiness vs. *BMEP* with various fuel mixtures (and water injection).

Pure hydrogen has been used in several research projects with the aim of reducing CO_2 emissions, because it could decrease the greenhouse gas releases of whole transport fleets. However, HHO gas does not significantly influence CO_2 emissions. The differences in measured CO_2 values with the use of hydroxygen were negligible in comparison to using solely diesel. The WI slightly increased CO_2 emissions by 0.1%. The volatility of the CO_2 data do not allow for making more clear statements and conclusions.

A decrease in CO emissions was registered in the tests with hydroxygen gas, but the addition of water increased CO emissions more than twofold at all ranges of loads (Figure 8). Carbon monoxide was released due to a known chain reaction [40]: $RH \rightarrow R \rightarrow RO_2 \rightarrow RCHO \rightarrow RCO \rightarrow CO$; here, *R* stands for the HC radical. The rate of this reaction cycle exponentially depends on temperature. The injection of HHO initiated faster combustion at the pre-mixed phase but led to a shorter combustion duration, reduced the *ROHR*, and oxidized more CO molecules; therefore, negligible increases in the CO were observed in the D+HHO mode.

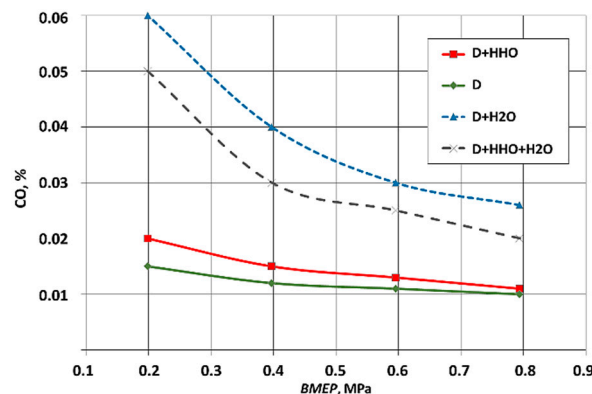


Figure 8. The CO vs. *BMEP* with various fuel mixtures (and water injection).

Injected water reduced the temperature, which significantly decreased the reaction rate and thus promoted the emission of CO. As mentioned previously, there is another reason for the increase in CO. The shortened auto-ignition delay with the injection of HHO reduced the *ROHR* and increased the cyclical amount of diesel. The combustion of a higher amount of diesel fuel generated more CO.

The increase in HC (Figure 9) was observed during tests of the D+HHO mode in comparison with the D mode. The HC emissions increased by 12–20% when the engine was fueled with the D+HHO mixture, as a result of the increased *BSFC*. The heating value of the stoichiometric HHO–air mixture was lower and the auto-ignition delay was shorter with D+HHO; therefore, *BSFC* increased and caused the increase in HC. When the engine

was fed with D+HHO+H₂O, hydrocarbon emissions were higher than those with D+HHO, but lower than those with D+H₂O.

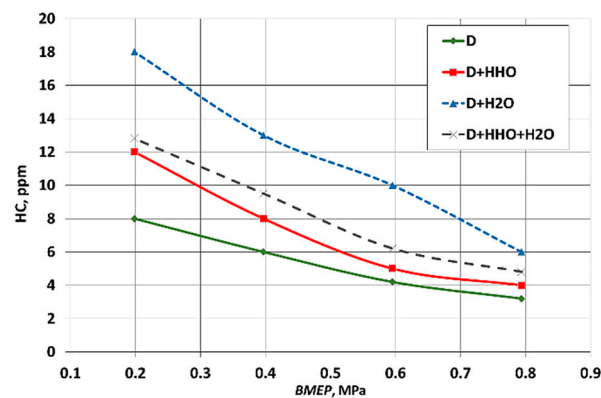


Figure 9. The HC vs. *BMEP* with various fuel mixtures (and water injection).

The injection of H₂O cooled the sucked air, eliminated the early ignition of H₂, and thus increased the auto-ignition delay. The injection of water decreased the combustion temperature and more unburned fuel fractions were emitted into the atmosphere. Evidence of this is the increase in HCs compared to D and D+HHO modes. The optimal results of HC and other emissions could be achieved by changing the amount of water supplied and the timing of the diesel fuel injections.

Formation of HCs as incomplete combustion fractions were mostly determined by OH and H radicals; thus, by the mass fractions of HHO and temperature. The water vapor reduced the temperature and speed of the flame in the combustion chamber. Due to the low quenching distance of HHO, partial combustion of the combustion mixture increased in the vicinity of cooler walls of the chamber, and thus increased the emissions of HCs.

3.3. AVL BOOST Simulation

The test engine model of AVL BOOST was developed in order to perform simulations of engine cycles and gas exchanges. The test engine model included cylinders, injectors, air filters, a catalyst, intercooler, turbocharger, etc., connected by pipe elements according to the AVL BOOST Users Guide [41]. The simulation was performed with an AVL BOOST two-zone combustion model created for an Audi/VW 1.9 TDI engine (Figure 10).

The BOOST simulation model could register the pressure, temperature, and air/fuel ratio at measuring points. These data signals were transmitted into BOOST actuators to manage the throttle position or vane position of the variable geometry turbocharger. The obtained results were exported into MS Excel software.

Together with engine cycle simulations, there are possible benefits of accomplishing co-simulation with other software packages, as well as the possibility of relatively easily implementing user-described models [42]. The fuel mass and energy exchange process of this engine, together with other engine systems, has been analyzed as an open thermodynamic system.

The intensity of *ROHR* of the working fluid during the cycle was determined with the Vibe's heat release function [43]:

$$\frac{dx}{d\phi} = -a \frac{m_v + 1}{\phi_c} \left(\frac{\phi}{\phi_c} \right)^{m_v} \exp \left[a \left(\frac{\phi}{\phi_c} \right)^{m_v + 1} \right] \quad (15)$$

where $dx = dQ/Q$; Q is the cyclic rate of heat release; ϕ is the crank angle from SOC; a is the efficiency parameter $a = -6.908$; m_v is the combustion intensity shape parameter; and ϕ_c is the CD.

The simulation revealed that the presence of HHO reduced the p_{max} , in comparison to the solely diesel mode. However, water injection positively assisted the co-combustion of D+HHO and p_{max} was higher (Figure 11). This could have been achieved due to the higher pressure rise, as the result of an increased diesel fuel mass flow rate (Table 9).

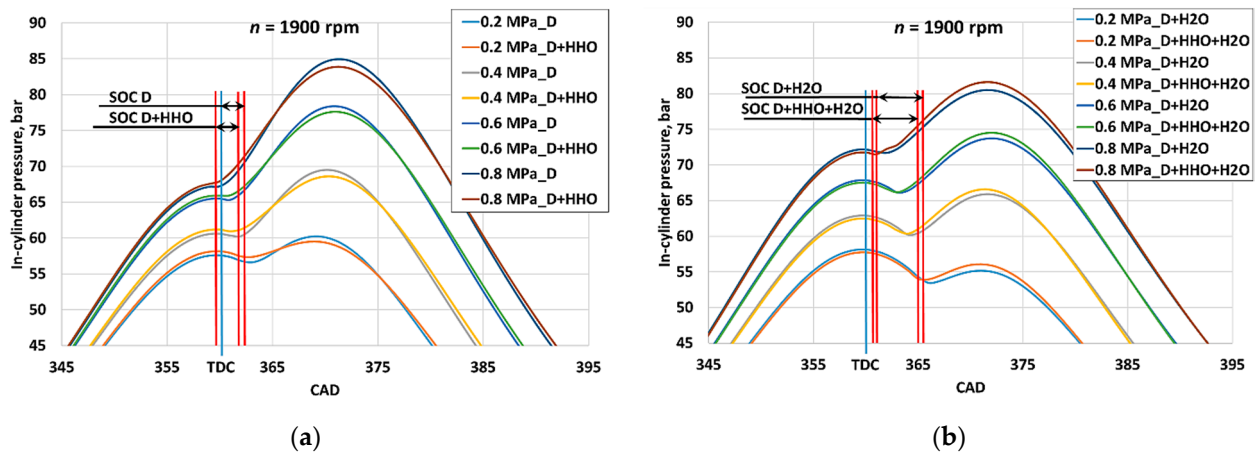


Figure 11. In-cylinder pressure vs. CAD for D and D+HHO modes (a), D+H₂O and D+HHO+H₂O modes at the various BMEP values (b).

More detailed findings are disclosed in relation to the SOC. The SOC in Figure 11 is depicted as a range (SOC D, SOC D+HHO, etc.), where combustion starts at the various loads (0.2–0.8 MPa). The SOC was determined after the AVL BOOST simulation. The pressure traces and positions of the SOC within the range of 50 CAD are depicted in Figure 11, which shows that when the engine ran in the D+HHO mode, the SOC was delayed by 0.3–0.47 CAD or the auto-ignition delay phase became shorter, in comparison with the D mode.

Comparing the engine pressure traces of D+H₂O to D, the SOC was later by 3 CAD at low load and 1.5 CAD at high load, because the evaporated water cooled the compressed air and auto-ignition delay increased. The presence of HHO led to the earlier SOC, which can be seen in Figure 11b, and shorter CD, which can be seen in Table 10.

Table 10. The indicators set for various modes in AVL BOOST software.

Indicators	D+HHO	D	D+HHO+H ₂ O	D+H ₂ O
<i>BMEP = 0.2 MPa</i>				
Combustion duration (CD), CAD	38	39	41	43
Shape parameter, m_v	0.48	0.62	0.38	0.41
<i>BMEP = 0.4 MPa</i>				
Combustion duration (CD), CAD	40	41	44	46
Shape parameter, m_v	0.54	0.67	0.44	0.47
<i>BMEP = 0.6 MPa</i>				
Combustion duration (CD), CAD	45	46	48	51
Shape parameter, m_v	0.60	0.67	0.54	0.59
<i>BMEP = 0.8 MPa</i>				
Combustion duration (CD), CAD	49	52	55	57
Shape parameter, m_v	0.67	0.69	0.61	0.65

SOC is related to the SOI, and with respect to its CAD positions, it represents the auto-ignition delay. The auto-ignition delay was assumed to be the distance from the position of SOI set during the test and the position of SOC identified with AVL BOOST (Figure 12). Figure 12 presents the positions of SOI and SOC at various *BMEP* values.

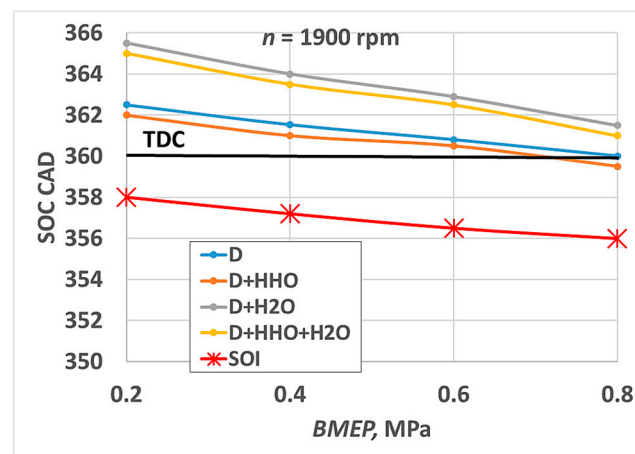


Figure 12. The SOI (set during the experiment) and SOC (determined by the AVL BOOST) vs. *BMEP*.

The auto-ignition delay with D+HHO+H₂O was shorter by 0.5 CAD in comparison with D + H₂O. This means that combustion started earlier and it was faster; consequently, the combustion duration (CD) was shorter (Table 10). These conditions could facilitate the higher p_{max} with D+HHO+H₂O than that of D+H₂O mode, as can be seen in Figure 11b.

It can be observed (Figure 12) that the more tangible influence on auto-ignition delay was caused by water injection. The auto-ignition delay was longer by 3 CAD at a *BMEP* of 0.2 MPa, by 2.5 CAD at a *BMEP* of 0.4 MPa, by 1.8–2.1 CAD at a *BMEP* of 0.6 MPa, and by 1.5 CAD at a *BMEP* of 0.8 MPa. However, relatively small amounts of HHO (0.0125 kg/h) shortened the auto-ignition delay by 0.3–0.5 CAD and SOC occurred earlier. Due to the faster combustion, increase of pressure, and the more advanced start of *ROHR* were noticed.

Injection of the HHO also resulted in a shorter combustion duration in comparison to the solely diesel fuel mode. The early start of the combustion process caused it to start to slow down at the premixed combustion phase, and further at the diffusion combustion stage. These phenomena were analyzed with Vibe's defined parameter combustion intensity shape parameter, m_v .

The shorter CD is related to the lower combustion intensity at the premixed combustion phase. This was proven by the increase in combustion intensity shape parameter m_v determined during the AVL BOOST simulation (Table 10). The higher intensity of combustion at the premixed phase indicated the lower m_v values of the combustion intensity, whereas the higher m_v values suggested the higher intensity in the middle or at the end of combustion. The combustion intensity shape parameter was lower in these cases when HHO facilitated a higher combustion intensity with an early start of combustion and a shorter auto-ignition delay in comparison with D or D+H₂O. However, combustion in this case was faster, and CD was made shorter (Table 10).

Pressure-rise graphs of all tested fuel mixtures over CAD are plotted in Figure 13. There two increasing slopes are observed in the graph of the in-cylinder pressure-rise curves. The first peak of the pressure-rise appeared in the vicinity of 347 CAD for all tested mixtures. At this point, the pressure-rise increased due to the volume change of the combustion chamber, caused by piston motion towards the TDC, and could be referred to as the volume change-affected pressure-rise. The following second and more sudden peaks of the pressure-rise lines were within the range of SOC and TDC, related to the main combustion phase of the 10–90% MFB with clearly expressed turbulent character.

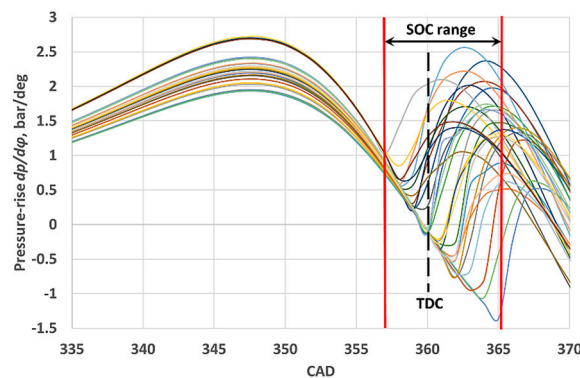


Figure 13. The pressure-rise graph of all tested fuel mixtures as function of CAD.

Detailed pressure-rise graphs with various fuel mixtures are depicted in Figure 14. The pressure rise affected by turbulent combustion was lower using the D+HHO mixture as compared to the D mode. The D+HHO mixture was more homogeneous, but seemed to be unable to achieve more intensive combustion and to reach a higher pressure-rise. The injection of water changed the trends of pressure-rise.

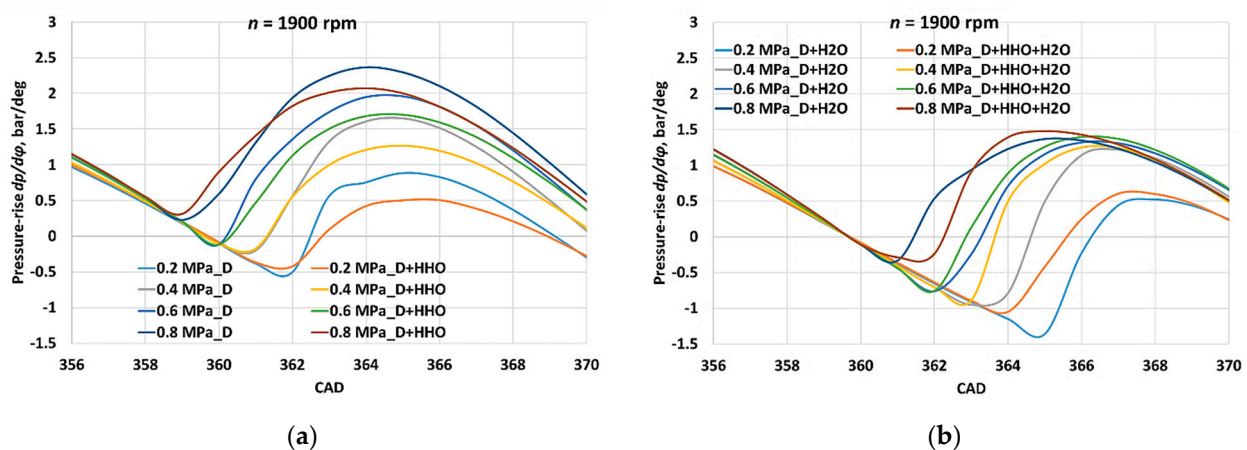


Figure 14. The pressure-rise $dp/d\phi$ vs. CAD for D and D+HHO modes (a), D+H₂O and D+HHO+H₂O modes at the various BMEP values (b).

The pressure-rise was higher by 10.9–22.7% with D+HHO+H₂O than that with D+H₂O; however, it was delayed by 2–3 CAD with the D+HHO+H₂O mode. Additionally, it can be observed that a combination of HHO and WI provides a higher pressure rise than HHO alone. The water droplets decreased the temperature, and because of turbocharger pressure, the density of the mixture increased; thus, the pressure-rise peak increased. Another reason could be that the whole D+HHO+H₂O mixture become more homogeneous, unless the temperature of mixture decreased and the pressure-rise started later, but HHO co-combusted with the diesel fuel more efficiently and pressure-rise reached a higher peak in comparison to the D+H₂O mode.

The *ROHR* values had correlated trends to those of pressure-rise to some extent. The *ROHR* decreased when engine was fueled with the D+HHO mixture by 0.99–1.98 J/deg (Figure 15a). A significant increase in the diesel fuel mass flow rate by 0.19–0.24 kg/h (Table 9) and a shortened auto-ignition delay led to a longer CD but lower *ROHR*.

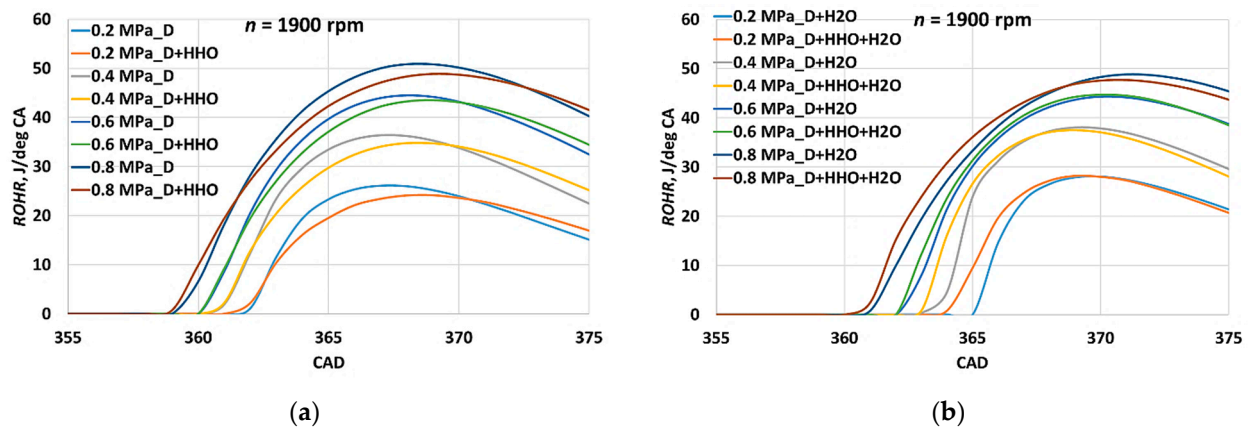


Figure 15. The $ROHR$ vs. CAD for D and D+HHO modes (a), D+H₂O and D+HHO+H₂O modes at the various $BMEP$ values (b).

The water injection positively affected the co-combustion of D+HHO. The water droplets contributed to increases in the density and homogeneity of the mixture, and the more intensive combustion, which is evidenced by the lower diesel fuel mass flow rate of 0.036–0.137 kg/h. The lower temperature of the mixture led to a longer auto-ignition delay, clearly seen in Figure 12. However, the peak of $ROHR$ reached approximately the same magnitude as that without HHO. The result of this simulation also evidenced that a combination of HHO with water injection produces a dense, homogenized mixture, suitable for achieving the sufficient performance parameters.

4. Conclusions

Tests were conducted with a turbocharged CI engine under dual-fuel mode using diesel fuel and HHO gas to study the effect of water injection on performance and emission indicators. The following conclusions have been drawn on the basis of the experiment and the results of the simulation:

1. Reductions in p_{max} , BTE and increases in $BSFC$ were observed with the D+HHO mode at all the $BMEP$ values. The injection of water lowered the temperature in the chamber, and the combustion mixture ignited later with D+H₂O and D+HHO+H₂O modes. The combination of HHO with water injection produced a dense, homogenized mixture, which could better achieve the desirable engine performance parameters;
2. The decrease in NO_x emissions in the D+HHO mode was very modest. NO_x emissions were reduced by 3–4%. The water injection (D+HHO+H₂O mode) decreased NO_x emissions at low loads more than twofold, and at high loads by 3–4-fold. Vaporization of the water reduced the temperature of the mixture, the CD increased, released heat reduced the combustion temperature, and the levels of NO_x emissions were significantly lowered;
3. A slight increase in CO emissions was registered during tests of D+HHO in comparison with the D mode. However, tests with D+HHO+H₂O showed that CO emissions increased at all ranges of loads. The injection of water led to a decrease in the CO oxidation reaction rate and an increase in CO emissions;
4. The influence of HHO on CO_2 emissions was negligible. Due to the injection of water (D+HHO+H₂O mode), CO_2 emissions slightly increased—by 0.1%;
5. The HC emissions increased by 12–20% when the engine was fueled with a D+HHO mixture. Due to the low heating value of the stoichiometric HHO–air mixture and shorter auto-ignition delay, the $BSFC$ and HC increased. Another reason for the increase in HC emissions is the low quenching distance of HHO. Combustion of the mixture occurred at the chamber walls, and thus increased the HC emissions. HC emissions were higher with D+HHO+H₂O in comparison with D and D+HHO.

6. The simulation of AVL BOOST revealed that the combustion started earlier with the use of HHO and the auto-ignition delay was shorter in comparison with solely D or D+H₂O modes, although combustion was faster and CD was shorter;
7. Combinations of HHO and WI injection can be used to diminish the NO_x emissions with slight decreases in the engine *BTE*.

The relatively low hydrogen energy fraction (0.65–1.8%) in the state of hydroxygen, in combination with water injection, resulted in substantial decreases in NO_x emissions at the ranges of loads. Hence, fueling a CI engine with hydroxygen supplied by an on-board water electrolyser is a promising solution for improvements of NO_x emissions from hybrid electric vehicles. However, to consider the overall efficiency and performance of CI engines, further experiments and life-cycle assessments should be performed with a higher HES. A substantial amount of hydroxygen can be generated using the batteries of hybrid vehicles.

Author Contributions: Conceptualization, R.J. and S.S.; methodology, A.R.; software, R.J.; validation, A.R.; formal analysis, R.J. and A.R.; investigation, R.J. and A.R.; resources, S.P.; data curation, R.J.; writing—original draft preparation, R.J.; writing—review and editing, S.S.; visualization, S.P.; supervision, S.P. All authors have read and agreed to the published version of the manuscript.

Funding: This research received no external funding.

Institutional Review Board Statement: Not applicable.

Informed Consent Statement: Not applicable.

Data Availability Statement: Not applicable.

Acknowledgments: The results of the research were obtained using a virtual internal engine simulation tool, AVL BOOST, acquired by signing a Cooperation Agreement between AVL Advanced Simulation Technologies and the Faculty of Transport Engineering of Vilnius Gediminas Technical University.

Conflicts of Interest: The authors declare no conflict of interest.

Abbreviations

The following abbreviations are used in this manuscript:

ABDC	After bottom dead center
ATDC	After top dead center
BBDC	Before bottom dead center
BTDC	Before top dead center
<i>BMEP</i>	Brake mean effective pressure
<i>BSFC</i>	Brake specific fuel consumption
<i>BTE</i>	Brake thermal efficiency
D	Diesel fuel
CA	Crank angle
CAD	Crank angle degree
CD	Combustion duration
CI	Compressed ignition
CNG	Compressed natural gas
CO	Carbon monoxide
CO ₂	Carbon dioxide
CR	Compression ratio
EGR	Exhaust gas recirculation
FC	Fuel cell
H ₂	Hydrogen
HC	Hydrocarbon
HES	Hydrogen energy share
HHO	Hydroxygen
IMEP	Indicated mean effective pressure
ICE	Internal combustion engine
ITE	Indicated thermal efficiency

LHV	Lower heating value
MFB	Mass fraction burned
NO _x	Nitrogen oxides
NTP	Normal temperature and pressure—defined as 20 °C and 101,325 kPa
PM	Particulate matter
ROHR	Rate of heat released
RME	Rapeseed methyl ester
STP	Standard temperature and pressure—defined as 273.15 K and 1 bar
SWC	Specific water consumption
SOI	Start of injection
SOC	Start of combustion
TDC	Top dead center
ULSD	Ultra-low-sulfur diesel
H ₂ O	Water
WI	Water injection
Symbols:	
m_v	Combustion intensity shape parameter
n	Engine speed
M_e	Engine torque
p	In-cylinder pressure
p_{max}	In-cylinder peak pressure
B_{H_2}	Mass flow rate of HHO
$dp/d\varphi$	Pressure-rise in the cylinder
Sm	Smokiness
vol	Volume
wt.	Weight

References

1. The International Council of Clean Transport. *European Vehicle Market Statistics*; Pocket Book: Lugano, Switzerland, 2014.
2. International Energy Agency Highlights. CO₂ Emissions from Fuel Combustion. Overview. 2017. Available online: <http://www.iea.org/publications/freepublications/publication/CO2EmissionsFromFuelCombustion2017Overview.pULSD> (accessed on 31 October 2017).
3. European Commission Decision C, 4614. Work Programme 2016–2017 “Smart, Green and Integrated Transport”, 2016. Brussels. 2016. Available online: <https://egvi.eu/wp-content/uploads/2019/07/WP-2016-2017-updated.pdf> (accessed on 19 September 2020).
4. Momirlan, M.; Veziroglu, T.N. The properties of hydrogen as fuel tomorrow in sustainable energy system for a cleaner planet. *Int. J. Hydrogen Energy* **2005**, *30*, 795–802. [CrossRef]
5. Tauzia, X.; Maiboom, A.; Shah, S.R. Experimental study of inlet manifold water injection on combustion and emissions of an automotive direct injection Diesel engine. *Energy* **2010**, *35*, 3628–3639. [CrossRef]
6. Barreto, L.; Makihira, A.; Riahi, K. The hydrogen economy in the 21st century: a sustainable development scenario. *Int. J. Hydrogen Energy* **2003**, *282*, 67–284. [CrossRef]
7. Rimkus, A.; Pukalskas, S.; Juknelevičius, R.; Matijošius, J.; Kriaučiūnas, D. Evaluating combustion, performance and emission characteristics of CI engine operating on diesel fuel enriched with HHO gas. *J. KONES Powertrain Transp.* **2018**, *25*, 2018. [CrossRef]
8. Saravanan, N.; Nagarajan, G.; Sanjay, G.; Dhanasekaran, C.; Kalaiselvan, K.M. Combustion analysis on a DI diesel engine with hydrogen in dual fuel mode. *Fuel* **2008**, *87*, 3591–3599. [CrossRef]
9. Szwaja, S. *Studium Pulszki Ciśnienia Spalania W Tłokowym Silniku Spalinowym Zasilanym Wodorem*; Wydawnictwo Politechniki Częstochowskiej: Częstochowa, Polska, 2010; 229p, ISBN 978-83-7193-459-9.
10. Perry, R.H.; Green, D.W. *Perry's Chemical Engineers' Handbook*, 7th ed.; McGraw-Hill: New York, USA, 1997; ISBN 0-07-049841-5.
11. Salvi, B.L.; Subramanian, K.A. Sustainable development of road transportation sector using hydrogen energy system. *Renew. Sustain. Energy Rev.* **2015**, *51*, 1132–1155. [CrossRef]
12. Verhelst, S.; Wallner, T. Hydrogen-fueled internal combustion engines. *Sci. Direct Prog. Energy Combust. Sci.* **2009**, *35*, 490–527. [CrossRef]
13. Gupta, R.B. *Hydrogen Fuel: Production, Transport and Storage*; Taylor & Francis Group: Boca Raton, FL, USA, 2009; 601p, ISBN 978-1-4200-4575-8.
14. Lewis, B.; von Elbe, G. *Combustion, Flames and Explosions of Gases*, 3rd ed.; Academic Press: New York, NY, USA, 1987.
15. Saravanan, N.; Nagarajan, G.; Narayanasamy, S. *Experimental Investigation on Performance and Emission Characteristics of DI diesel Engine with Hydrogen Fuel*; SAE Technique Paper; SAE International: Warrendale, PA, USA, 2007.
16. Gomes Antunes, J.M.; Mikalsen, R.; Roskilly, A.P. An experimental study of a direct injection compression ignition hydrogen engine. *Int. J. Hydrogen Energy* **2009**, *34*, 6516–6522. [CrossRef]

17. Zhou, J.H.; Cheung, C.S.; Leung, C.W. Combustion, performance, regulated and unregulated emissions of a diesel engine with hydrogen addition. *Appl. Energy* **2014**, *126*, 1–12. [[CrossRef](#)]
18. Karagoz, Y.; Sandalci, T.; Yuksek, L.; Dalkilic, A.S. Engine performance and emission effects of diesel burns enriched by hydrogen on different engine loads. *Int. J. Hydrogen Energy* **2015**, *40*, 6702–6713. [[CrossRef](#)]
19. Juknelevičius, R.; Szwaja, S.; Pyrc, M.; Gruca, M. Influence of hydrogen co-combustion with diesel fuel on performance, smoke and combustion phases in the compression ignition engine. *Int. J. Hydrogen Energy* **2019**. [[CrossRef](#)]
20. Juknelevičius, R.; Rimkus, A.; Pukalskas, S.; Matijošius, J. Research of performance and emission indicators of the compression-ignition engine powered by hydrogen—Diesel mixtures. *Int. J. Hydrogen Energy* **2019**. [[CrossRef](#)]
21. Cloonan, M.O. A chemist’s view of J.M. Calo’s comments on: “A new gaseous and combustible form of water” by R.M. Santilli (Int. J. Hydrogen Energy 2006, 31, 1113–1128). *Int. J. Hydrogen Energy* **2008**, *33*, 922–926. [[CrossRef](#)]
22. Santilli, R.M. A new gaseous and combustible form of water. *Int. J. Hydrogen Energy* **2006**, *31*, 1113–1128. [[CrossRef](#)]
23. Yilmaz, A.C.; Uludamar, E.; Aydin, K. Effect of hydroxy (HHO) gas addition on performance and exhaust emissions in compression ignition engines. *Int. J. Hydrogen Energy* **2010**, *35*, 11366–11372. [[CrossRef](#)]
24. Arat, H.T.; Baltacioglu, M.K.; Ozcanli, M.; Aydin, K. Effect of using Hydroxy and CNG fuel mixtures in a non-modified diesel engine by substitution of diesel fuel. *Int. J. Hydrogen Energy* **2016**, *41*, 8354–8363. [[CrossRef](#)]
25. Premkartiikumar, S.R.; Annamalai, K.; Pradeepkumar, A.R. Effectiveness of oxygen enriched hydrogen-hho gas addition on direct injection diesel engine performance, emission and combustion characteristics. *Therm. Sci.* **2014**, *18*, 259–268. [[CrossRef](#)]
26. Masjuki, H.H.; Ruhul, A.M.; Mustafi, N.N.; Kalam, M.A.; Arbab, M.I.; Rizwanul Fattah, I.M. Study of production optimization and effect of hydroxyl gas on a CI engine performance and emission fueled with biodiesel blends. *Int. J. Hydrogen Energy* **2016**, *41*, 14519–14528. [[CrossRef](#)]
27. Rimkus, A. Improvement of Efficiency of Operation of an Internal Combustion Engine by Using Brown’s Gas. Ph.D. Thesis, Technological Sciences, Transport Engineering (03T), Vilnius Gediminas Technical University, Technika, Vilnius, Lithuania, 2013.
28. Baltacioglu, M.K.; Arat, H.T.; Ozcanli, M.; Aydin, K. Experimental comparison of pure hydrogen and HHO (hydroxy) enriched biodiesel (B10) fuel in a commercial diesel engine. *Int. J. Hydrogen Energy* **2016**, *41*, 8347–8353. [[CrossRef](#)]
29. Mustafa, O.; Mustafa, A.A.; Ahmet, C.; Hasan, S. Using HHO (Hydroxy) and hydrogen enriched castor oil biodiesel in compression ignition engine. *Int. J. Hydrogen Energy* **2017**, *42*, 1–7.
30. Rimkus, A.; Pukalskas, S.; Matijošius, J.; Sokolovskij, E. Betterment of ecological parameters of a diesel engine using Brown’s gas. *J. Environ. Eng. Landsc. Manag.* **2013**, *21*, 133–140. [[CrossRef](#)]
31. Tesfa, B.; Mishra, R.; Gu, F.; Ball, A.D. Water injection effects on the performance and emission characteristics of a CI engine operating with biodiesel. *Renew. Energy* **2012**, *37*, 333–344. [[CrossRef](#)]
32. Adnan, R.; Masjuki, H.H.; Mahlia, T.M.I. Performance and emission analysis of hydrogen fueled compression ignition engine with variable water injection timing. *Energy* **2012**, *43*, 416–426. [[CrossRef](#)]
33. Chinatala, V.; Subramanian, K.A. Hydrogen energy share improvement along with NO_x emission reduction in a hydrogen dual-fuel compression ignition engine using water injection. *Energy Convers. Manag.* **2014**, *83*, 249–259. [[CrossRef](#)]
34. Chinatala, V.; Subramanian, K.A. Experimental investigation of hydrogen energy share improvement in a compression ignition engine using water injection and compression ratio reduction. *Energy Convers. Manag.* **2016**, *108*, 106–119. [[CrossRef](#)]
35. Taghavifar, H.; Anvari, S.; Parvishi, A. Benchmarking of water injection in a hydrogen-fueled diesel engine to reduce emissions. *Int. J. Hydrogen Energy* **2017**, *42*, 11962–11975. [[CrossRef](#)]
36. Holman, J.P. *Experimental Methods for Engineers*, 8th ed.; McGraw-Hill: New York, NY, USA, 2011; ISBN 978-0-07-352930-1.
37. Miyamoto, T.; Hasegawa, H.; Mikami, M.; Kojima, N.; Kabashima, H. Effect of hydrogen addition to intake gas on combustion and exhaust emission characteristics of a diesel engine. *Int. J. Hydrogen Energy* **2011**, *36*, 13138–13149. [[CrossRef](#)]
38. Lee, T.; Park, J.; Kwon, S.; Lee, J.; Kim, J. Variability in operationbased NO_x emission factors with different test routes, and its effects on the real-driving emissions of light diesel vehicles. *Sci. Total Environ.* **2013**, *461–462*, 377–385. [[CrossRef](#)] [[PubMed](#)]
39. Prabhakumar, G.P.; Swaminathan, S.; Nagalingam, B.; Gopalakrishnan, K.V. Water induction studies in a hydrogen-diesel dual-fuel engine. *Int. J. Hydrogen Energy* **1987**, *12*, 177–186. [[CrossRef](#)]
40. Heywood, J.B. *Internal Combustion Engine Fundamentals*; Mc’Graw-Hill Education: New York, NY, USA, 2018; 1028p, ISBN 9781260116106.
41. AVL BOOST. *Users Guide*; AVL LIST GmbH: Graz, Austria, 2011; 297p.
42. Alqahtani, A.; Shokrollahihassanbarough, F.; Wyszynski, M.L. Thermodynamic simulation comparison of AVL BOOST and Ricardo WAVE for HCCI and SI engines optimisation. *Combust. Engines* **2015**, *161*, 68–72. [[CrossRef](#)]
43. Vibe, I.I. *Brennverlauf und Kreisprozeß von Verbrennungsmotoren*; Verlag Technik: Berlin, Germany, 1970; 286p.